

**ARTICLE**

# Zeolite A Synthesized from Geothermal Waste Using Conventional and Microwave Heating for the Hydrothermal Treatment

Sulardjaka Sulardjaka<sup>1,\*</sup>, Sri Nugroho<sup>1</sup>, Norman Iskandar<sup>1</sup>, Agus P. Adi<sup>1</sup> and Deni F. Fitriyana<sup>2</sup>

<sup>1</sup>Diponegoro University, Semarang, 50275, Indonesia

<sup>2</sup>Universitas Negeri Semarang, Gunungpati, Semarang, 50229, Indonesia

\*Corresponding Author: Sulardjaka Sulardjaka. Email: sulardjaka@lecturer.undip.ac.id

Received: 29 May 2020 Accepted: 24 December 2020

**ABSTRACT**

Zeolite A has been successfully synthesized from geothermal waste with sodium aluminate and sodium silicate using conventional (C-H) and microwave heating (M-H) for the hydrothermal treatment. The products obtained for different aging times have been characterized using X-Ray Diffraction (XRD), Fourier transformation infrared spectroscopy (FTIR), and scanning electron microscopy (SEM). It is shown that with the M-H process, zeolite can be formed at relatively low temperature (100°C) in a relatively short time (40 min). The crystallization of zeolite A has been found to be generally promoted by an increase of aging and synthesis time; however, it has also been observed that relative long aging times can transform it into sodalite. Zeolite A produced through the M-H process generally displays a smaller and more homogeneous crystal size with respect to that obtained with the C-H method.

**KEYWORDS**

Geothermal waste; microwave-hydrothermal; conventional-hydrothermal; zeolite A

## 1 Introduction

Geothermal energy is heat that generated or comes from the sub-surface of the earth. The geothermal energy produces heat and can be used as a resource in power plant generation. In the production process, wastes are produced (geothermal sludge and brine) in large quantities, and are the byproducts from power plants, in which the water and steam extracted from the underground are used to generate electricity [1,2].

Zeolites are crystals consisting of aluminate and silicate frameworks, with the ability to act as catalysts, adsorbents, etc. As a consequence of their properties, they have many potential applications in the fields of petrochemical reactions, water and gas purification [3–5]. Zeolite A is a type of zeolites, and due to its large ion exchange capacity, mechanical strength, and particular crystal shape, it is used in the substitution of sodium tripolyphosphate in the aspect of detergent and water softening.

In the synthesis of zeolite A, sodium silicate and sodium aluminate are the most commonly used Si and Al resources. One of the problems in zeolite synthesis is the unavailability and cost of raw material, specifically the silica source. In order to reduce the production cost of synthesized zeolite, many alternative materials, such as silica source have been proposed. Some natural minerals and wastes, such as clinoptilolite, oil shale, municipal solid, rice husk and coal fly ash were used to replace sodium silicate in the synthesis of zeolite A for cost-saving and environmental protection purposes [6–11]. Geothermal



waste has high potential to be used as an alternative silica source for the synthesis of zeolite A, due to its silica contents. In previous study, by a conventional-hydrothermal process, geothermal waste was successfully converted into zeolite A and sodalite [12]. Colloidal silica extracted from geothermal fluid was synthesized to low Si/Al zeolite Y, with similarity characteristics compared to those prepared from a conventional silica sol or Ludox [13]. Hydrothermal process at 150°C for 5 h with 3 M of NaOH produced Zeolite X with octahedral crystal shape, having a specific surface area of 68.985 m<sup>2</sup>/gr and a pore volume of 0.109 cc/gr. The synthesized zeolite was successfully used as a catalyst for enhancing biohydrogen production [14,15]. The colloidal silica extracted from geothermal fluids is used as silica source for zeolite synthesis [16]. The purity and yield of zeolite A synthesized from natural minerals and wastes using hydrothermal treatment were limited to the SiO<sub>2</sub> extraction. In order to increase the yield of SiO<sub>2</sub> and synthetic zeolite, several methods, such as calcining, alkali, and acid activation were conducted to treat these raw materials before the synthesis process [12,17].

Several synthesis methods have been proposed for increasing the yield and purity of zeolite, besides conventional hydrothermal, some synthetic zeolites by microwave hydrothermal were produced. Also, numerous studies on the subject of microwave-hydrothermal (M-H) synthesis of zeolites have been published [9,18,19]. This research explained that the application of microwaves on zeolite synthesis, yield significant reduction in crystallization time due to faster and homogeneous heating, compared to conventional-hydrothermal (C-H) method. However, the fast temperature rise induced in the reacting solution by microwaves affects the nuclei formation, leading to the crystallization of undesired phases, or to the precipitation of amorphous solids [20,21]. The addition of seeds or ageing the solution were proved to bring a beneficial effect to nucleation in microwave synthesis of various zeolites [22]. Chu et al. [23] was the first to show that microwave heating is used for the rapid synthesis of zeolites, and the crystallization of zeolite NaA was obtained in 12 min, contaminated with hydroxysodalite (HS), even when the mixture was aged for 2 h at room temperature before the M-H treatment. Slangen et al. [24] obtained pure zeolite A in 5 min crystallization, and after 20 h of ageing at room temperature. While the product with little hydroxysodalite was obtained in as short as 4 h of ageing. In a laboratory scale, the microwave zeolite synthesis usually consists a batch reaction carried out in an autoclave made of a material transparent to microwaves, irradiated at 2.45 GHz in a multimodal oven cavity, similar to the customary household type [19,25].

This study used calcined geothermal waste as silica sources in synthesizing zeolite A. This waste was added into alkali solution and aluminum source, followed by microwave-hydrothermal (M-H) and conventional-hydrothermal (C-H) method. The ageing effects and crystallization time, on the formation of zeolite A were also investigated.

## 2 Materials and Methods

Geothermal waste from geothermal power plant was dried under the sunlight and sieved with a 320-mesh sieving machine. The powder was calcined by burning at 850°C for 3 h at atmospheric condition using Carbolite furnace. Calcining process was carried out to burn unexpected or volatile materials. The chemical compositions of geothermal waste before and after calcining were characterized by atomic absorption spectroscopy (AAS) using Shimadzu type AA-6650 and the results were presented in the form of stable oxides as shown in Tab. 1.

The first step for zeolite synthesis was making sodium silicate. In this research, sodium silicate was made from 3 gr of geothermal waste mixed with 30 mL of NaOH 5 M. These mixtures were stirred at 100°C for 20 min. Then, sodium aluminate was made from 20 g of NaOH 5 M dissolved in distilled water to yield 100 ml of 5 M NaOH, and then added 9 gr of Al(OH)<sub>3</sub> gradually, while stirring at 100°C for 20 min. The two suspensions: 30 mL of sodium silicate and 30 mL of sodium aluminate were mixed and stirred using a magnetic stirrer at 200 rpm for 2 h and 5 h ageing time at room temperature. The moment the silica

was added, it was taken as the beginning of ageing. This included the dissolution of silica in alumina solution [22], from this step resulted precursor gel for zeolite A synthesis.

**Table 1:** Chemical composition of geothermal powder

Compound	Before Calcining (wt.%)	After Calcining (wt.%)
Al <sub>2</sub> O <sub>3</sub>	0.055	0.142
Fe <sub>2</sub> O <sub>3</sub>	0.192	0.451
Na <sub>2</sub> O <sub>3</sub>	0.609	0.760
SiO <sub>2</sub>	49.100	80.043

A household-type microwave oven 2.45 GHz (Panasonic NN-SM320M) with maximum output power 450 Watt was used for microwave synthesis. For measuring the temperature of the process, the thermocouple was inserted into the microwave. The precursor gel was poured into a Teflon(R) box and placed into the microwave and heated at 100°C for 20, 40, and 60 min. The Teflon(R) autoclave with controllable heating was used for conventional hydrothermal process. This was performed by pouring the precursor gel into the Teflon(R) autoclave and heated until 100°C with holding time 3 h, 4 h, and 5 h. The synthesized products were washed with aquabidest and filtered with whatmann 42 paper to separate between solid and filtrate. The solid powder was dried in the oven at 80°C for 4 h. The powders were analyzed by Rigaku X-ray diffractometer using CuK $\alpha$  radiation (40 kV, 30 mA), 8201PC Shimadzu FTIR (Fourier Transform Infra-Red) and JEOL JSM 6300 SEM (Scanning Electron Microscope).

### 3 Results and Discussions

Tab. 1 shows that the geothermal powder before calcining contains 49.10% SiO<sub>2</sub>, and after, it increases up to 80.04 %. Munfarida et al. has reported that using EDX analysis geothermal waste form power plant has SiO<sub>2</sub> containing 35.09% and Al<sub>2</sub>O<sub>3</sub> about 0.05% [26]. Calcining process causes unexpected and volatile materials to burned out. While the calcined geothermal waste produced Si/Al ratio 1.79 as shown on Tab. 2. This ratio allows the formation of zeolite A, which according to the literature that this product has a ratio of Si/Al ranging from 1–3.5 [21]. Sulardjaka et al. [12] reported that the geothermal powder before calcining contained silica in amorphous form, there was no dominant peak from the diffractogram. However, the peaks were found at 21.91 and 20.88 in the calcined geothermal powder. This indicated that there was transformation of amorphous silica into primary cristobalite. During the calcining process until 850°C for 3 h, some of the silica transformed into cristobalite phase, and the amorphous silica phase was still dominant [27,28]. SiO<sub>2</sub> in amorphous form in geothermal waste has potential as a silica resources for zeolite synthesis.

**Table 2:** Si/Al ratio of synthetic mixture

Sample	Element	Average (wt.%)
Precursor gel	Al	5.86
	Si	10.48

XRD diffraction pattern of synthesized products from microwave-hydrothermal of geothermal waste for 2 h and 5 h ageing time were shown at Figs. 1 and 2, respectively. The phases produced from conventional-hydrothermal were shown in Fig. 3. The diffractogram pattern as shown in Figs. 1–3, correlated with that from JCPDS data number 11-0401 (hydroxy-sodalite) and 31-1269 (zeolite A). This showed that the

synthetic zeolite in all the variation contained crystal of zeolite A and sodalite. During the microwave-hydrothermal for 2 h ageing, holding time for 20 min, phase zeolite A became the dominant. While increasing the holding time to 40 and 60 min, the zeolite A also increased and sodalite phase was formed. X-Ray diffraction of microwave-hydrothermal of geothermal waste for 5 h ageing showed that at the ageing of 20 and 40 min, zeolite A phase was dominant. The rise of holding time to 60 min, increased the zeolite A and produced sodalite phase.

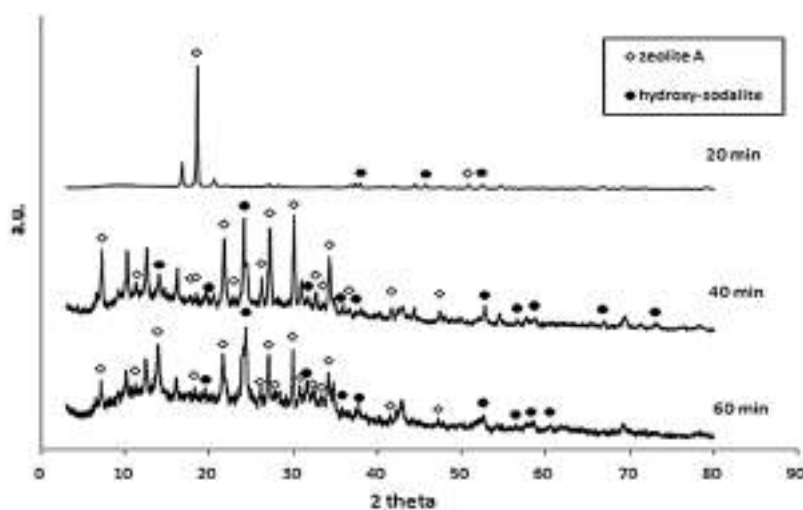


**Figure 1:** X-Ray diffraction of microwave-hydrothermal of geothermal waste for 2 h ageing with the variation of holding time

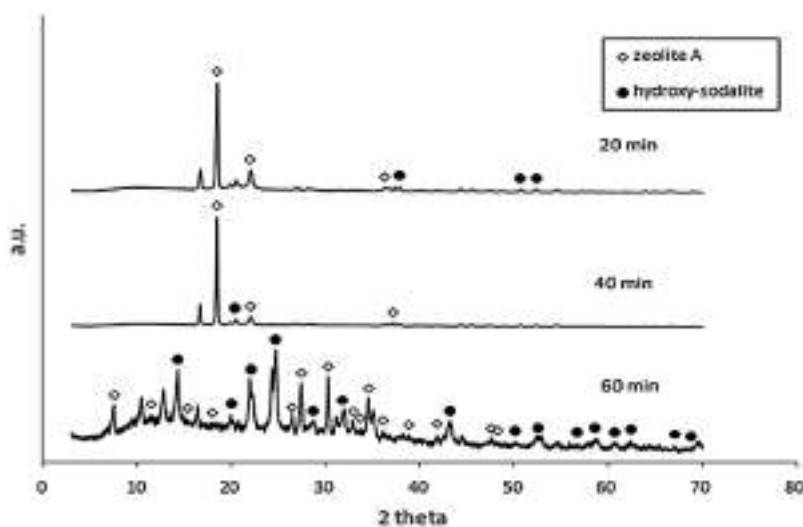


**Figure 2:** X-Ray diffraction of microwave-hydrothermal of geothermal waste for 5 h ageing with the variation of holding time

Fig. 3 showed X-Ray diffraction of conventional-hydrothermal of geothermal waste for 2 h ageing with 3 h, 4 h, 5 h holding time. At the holding time of 3 h, zeolite A and less sodalite phase were produced. The rise of holding time, increased zeolite A and sodalite phases. The holding time for 5 h hydroxy-sodalite phase was dominant. The microwave-hydrothermal (M-H) and conventional-hydrothermal (C-H) of geothermal

waste produced synthetic zeolite. Zeolites A and sodalite were produced in all of the variation of microwave-hydrothermal processes. The increasing M-H time, elevated the production of zeolite A and sodalite. However, the increasing C-H time, decreased the zeolite A phase and raised that of sodalite. In zeolite A synthesis, the formation of building units and the nucleation of zeolite with it, was followed by crystal growth by adsorption of the units on the surface of the zeolite nuclei and crystal. At the longer holding time, the impurity phase of zeolite A was formed. There has been a transformation from zeolite A  $\rightarrow$  sodalite. At the surface-to-core extension of crystallization, sodalite nanoplates were crystallized within the amorphous cores of zeolite A. At the longer holding time, sodalite nanoplates increased in size and breaking the cubic shells of zeolite A in the process. This led to the phase transformation from zeolite A to sodalite [28–30].

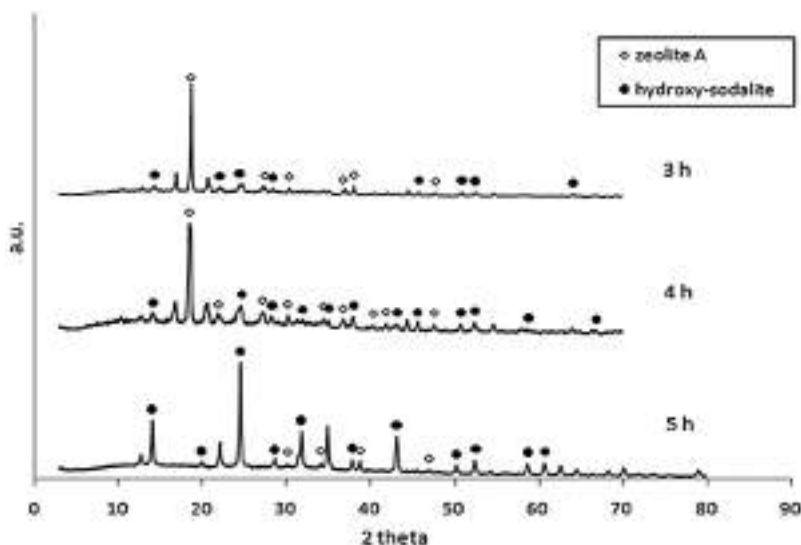


**Figure 3:** X-Ray diffraction of conventional-hydrothermal of geothermal waste for 2 h ageing with variation of holding time

The average of crystal grain size of synthesized zeolites was determined from the results of XRD graphs, this was calculated using Scherer formula [31,32].

$$L = \frac{57.3 \times k \times \gamma}{\beta \times \cos \theta} \quad (1)$$

where:

$L$  = crystal grain size (nm),

$k$  = oxide constant (0.94),

$\lambda$  = X-ray wavelength (1.5406 Å),

$\beta$  = the value of FWHM (deg),

$\theta$  = angle of crystal diffraction peak position (deg),

57.3 = correction factor from degree to radian.

The results of the crystal grain size calculation using Scherer formula was shown in Fig. 4. The crystal size of zeolite A produced from M-H were 13.43 nm (ageing 2 h) and 14 nm (ageing 5 h). The C-H with 2 h ageing produced zeolite A with crystal size of 53.94 nm, and sodalite of 35.4 nm. The sodalite with crystal size of 10.78 nm (ageing 2 h) and 11.38 nm (ageing 5 h) were also formed from M-H. The M-H produced

smaller and more homogeneous crystal size of zeolite A and sodalite, due to faster and homogeneous heating compared to the C-H. Ageing time with variation of 2 h and 5 h on the M-H method affected nucleation and crystallization of synthetic zeolite. The ageing of precursor gels resulted in the acceleration of the crystallization and crystal size diminution of the synthesis product. This ageing process directly influenced the concentration and number of formed nuclei [33]. The fast crystallization on M-H method affected the significant reduction of its time, 3 or 4 times, shorter than that of C-H method. It was also observed that the time and temperature of microwave heating had significant effects on the prepared zeolite particles. The shortening of synthesis times in microwave heating was caused by two different mechanisms, i.e., the rapid heat-up of the sample and a better heat transfer which resulted in the rapid and thorough heating of the synthesis mixture. This easily resulted in rapid and vivid heating of the synthesis mixture and effect a faster crystallization [34,35].

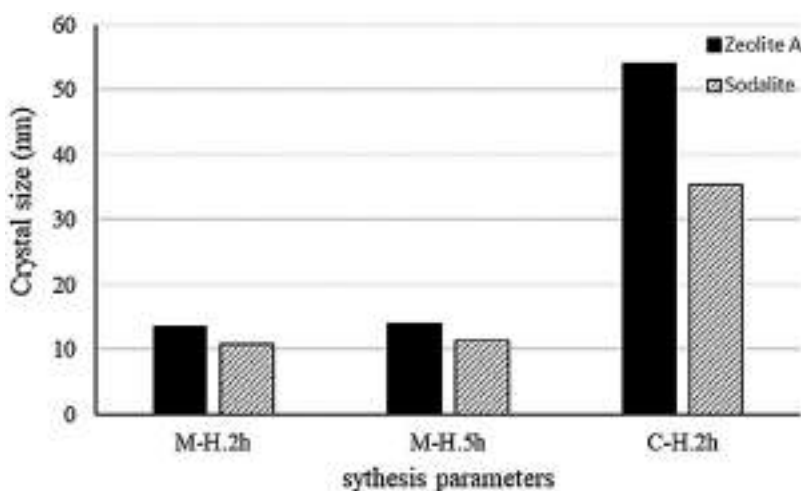


**Figure 4:** Crystal size of zeolite A and hydroxy-sodalite

FTIR analysis was conducted to identify the functional group on the synthetic zeolite. The data were analyzed based on the Nicodom FTIR Spectra Libraries. These data were obtained from references, such as the general FTIR vibrational region  $300\text{--}400\text{ cm}^{-1}$  (vibrations of the external opening of the pores caused by breathing motion of the ring hole 12),  $420\text{--}500\text{ cm}^{-1}$  (Si-O/Al-O bending vibrations),  $500\text{--}650\text{ cm}^{-1}$  (double ring D4R/ D6R external vibration) which showed the formation of zeolite A,  $650\text{--}850\text{ cm}^{-1}$  (symmetric stretching vibrations of O-Si-O or O-Al-O),  $900\text{--}1250\text{ cm}^{-1}$  (asymmetric stretching vibrations of O-Si-O or O-Al-O),  $1600\text{--}1700\text{ cm}^{-1}$  (O-H bending vibration) which showed the presence of zeolitic water ( $\text{H}_2\text{O}$ ), and  $3400\text{--}3700\text{ cm}^{-1}$  (O-H stretching vibration of Si-OH) [21]. The FTIR spectra of zeolite synthesis which resulted at 3 variations was shown in Figs. 5, 6, and 7.

There were wavenumber  $555.5\text{ cm}^{-1}$  and  $563.21\text{ cm}^{-1}$  for 40 and 60 min of 2 h ageing using the M-H method. The existence of absorption band in the region around  $500\text{--}650\text{ cm}^{-1}$  showed the double ring D4R or D6R. It was observed that zeolite A was only formed in variation for 40 and 60 min of 2 h ageing using the M-H method. There was only wavenumber  $563.21\text{ cm}^{-1}$  for 60 min of 5 h ageing with M-H. It was also found that zeolite A was only formed in variation for 60 min of 5 h ageing with M-H. There were wavenumbers of  $555.5\text{ cm}^{-1}$  and  $555.5\text{ cm}^{-1}$  for 3 h and 4 h of the 2 h ageing with C-H. The FTIR analysis was matched with the XRD test, that zeolite A was only formed in variation 3 h and 4 h of the 2 h ageing with C-H.

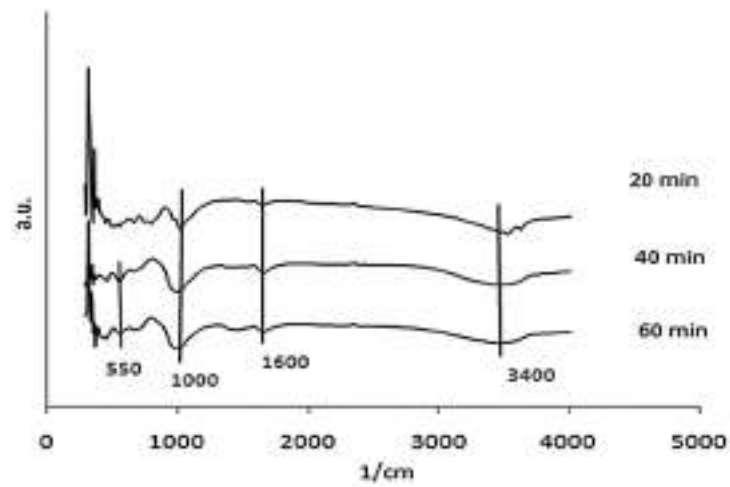


**Figure 5:** FTIR spectra of zeolite produced from microwave-hydrothermal synthesis for 2 h ageing

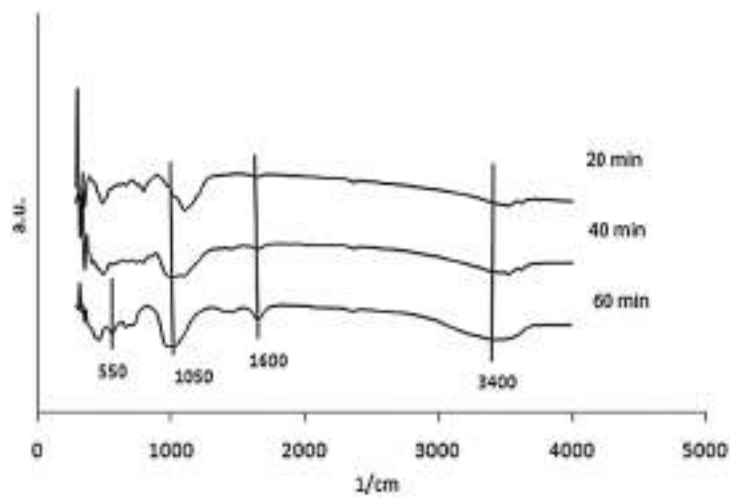


**Figure 6:** FTIR spectra of zeolite produced from microwave-hydrothermal synthesis for 5 h ageing

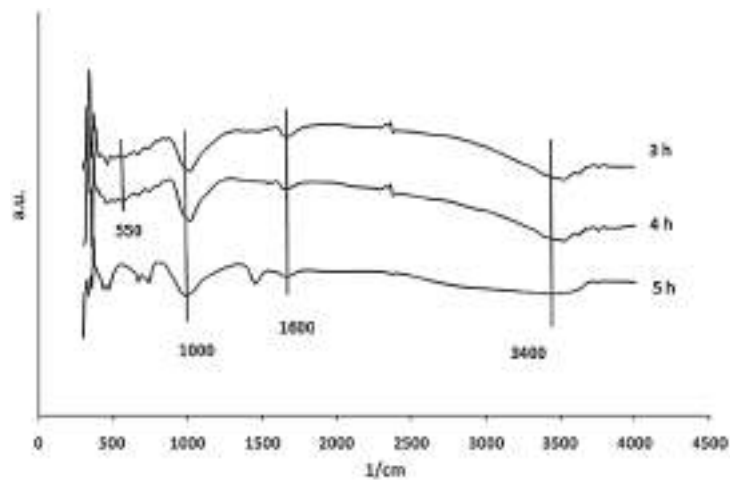


**Figure 7:** FTIR spectra of zeolite produced from conventional-hydrothermal synthesis for 2 h ageing

Scanning electron micrograph of the M-H process for 2 h ageing with holding time of 20, 40, and 60 min were shown in Figs. 8a, 8b, and 8c, respectively. It was shown that on variation 20 min, the formation of grain was not regular, while amorphous and zeolite A has not been formed yet. However, on variation 40 and 60 min, zeolite A and sodalite were formed. Zeolite A has cubic while sodalite has spherical form with an array of long fibers that surrounded it. The same with M-H for the ageing of 2 h and 5 h and the holding time of 20 min. The zeolite A formed, as shown in Fig. 6d. that the formation of grain was not regular or amorphous. The spherical form appeared on variation of 40 min (Fig. 6e), and showed that amorphous silica transformed into a crystal of zeolite. On variation of 60 min (Fig. 6f), the image showed the formation of many cubes, in the form of zeolite A and sodalite, has spherical form with an array of long fibers that surround it. The grain size of zeolite A and sodalite we are approximately 1  $\mu\text{m}$ .

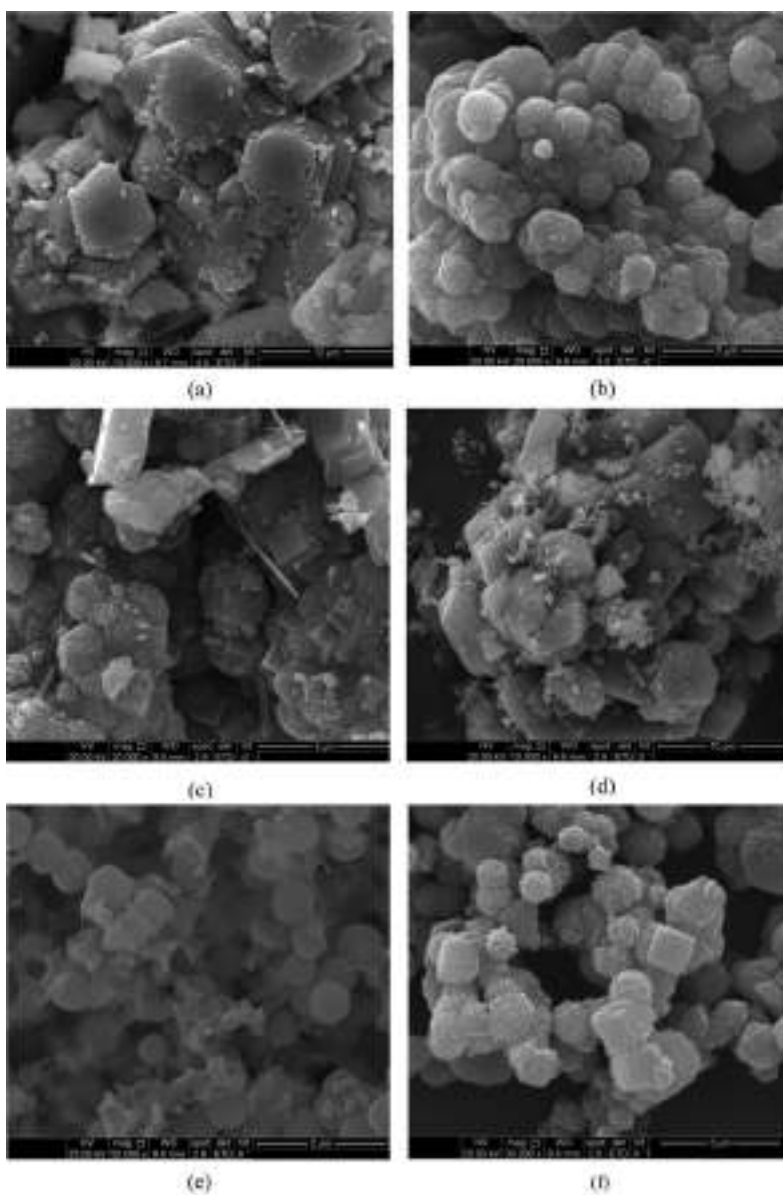


**Figure 8:** SEM image of synthetic zeolite for 2 h ageing with M-H (a) 20 min (b) 40 min (c) 60 min and 5 h (d) 20 min (e) 40 min (f) 60 min



The result of the SEM on the variation of 2 h ageing with C-H was shown in Fig. 9. On variation 3 h, the formation of zeolite A and sodalite with a grain size of about 5  $\mu\text{m}$  and 10  $\mu\text{m}$ , respectively were observed (Figs. 9a and 9b). Fig. 9a showed that there was a cubic formation of zeolite A. Fig. 9b showed sodalite phase. While Fig. 9c indicated that the formation of zeolite A and sodalite was not clear on variation 4 h, and only sodalite phase was observed, because zeolite A has been transformed into sodalite (Fig. 9d). The M-H produced smaller and more homogeneous grain size of zeolite A and sodalite, due to faster and homogeneous heating compared to C-H. The formation of sodalite as a side product in the synthesis of NaA was explained by the inadequate mixing. The prolonged heating resulted in the dissolution and regrowth of crystals composition, e.g., when a NaA mixture moved into a HS range, eventually, all NaA were transformed into sodalite. However, when the synthesis mixture stayed in the NaA region, the only sodalite that nucleated was in the inhomogeneous pockets [33].

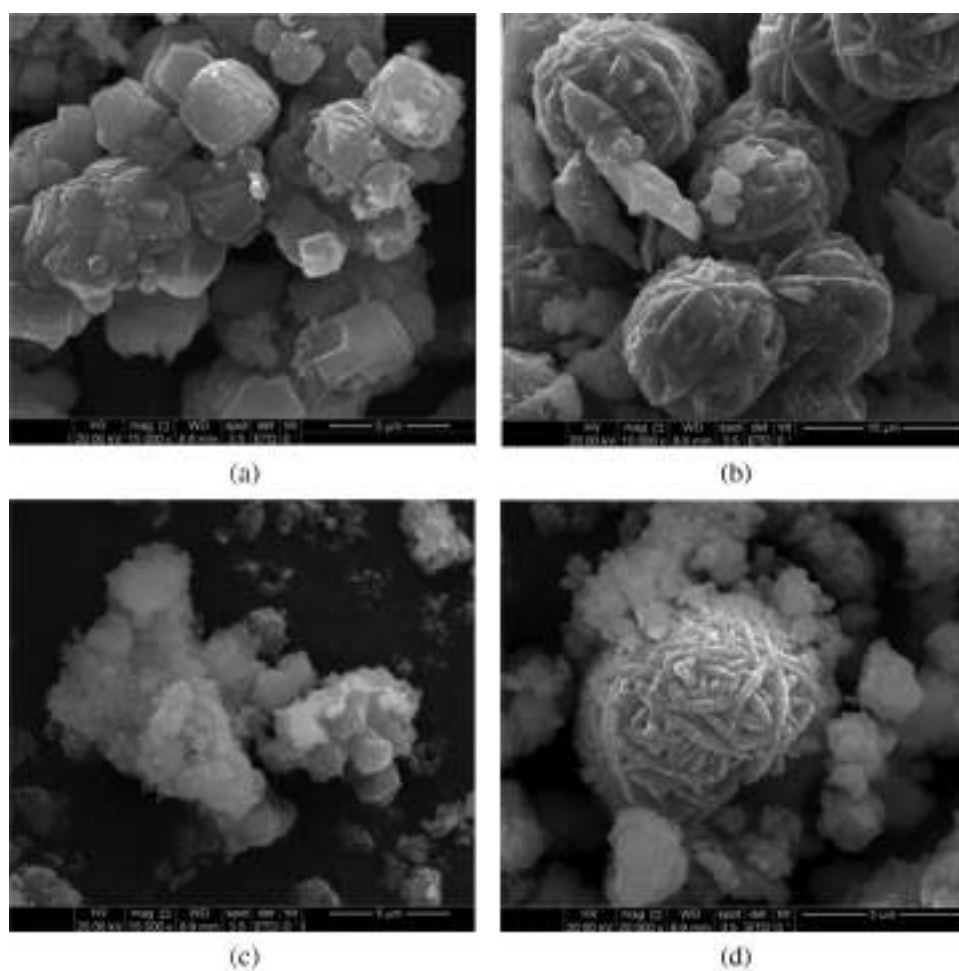


**Figure 9:** SEM image of synthetic zeolite 2 h ageing with C-H (a) 3 h zeolite A (b) 3 h sodalite (c) 4 h (d) 5 h

#### 4 Conclusions

Zeolite A was successfully synthesized from geothermal waste by conventional-hydrothermal (C-H) and microwave-hydrothermal (M-H) methods. This waste consists of 80.04%  $\text{SiO}_2$  and 0.142%  $\text{Al}_2\text{O}_3$ , while its silica content has high potential as an alternative source for synthesizing zeolite A. The rise of M-H and C-H time increased and decreased the crystallinity of zeolite A and sodalite, respectively. The fast crystallization

observed using the M-H method affected the significant reduction in duration to 3 or 4 times shorter, producing smaller and more homogeneous crystal size compared to the C-H method.

**Funding Statement:** This research was funded by the International Publication research grant, Diponegoro University, with the Contract No. 385-90/UN7.P4.3/PP/2018.

**Conflicts of Interest:** The authors declare no conflicts of interest regarding this study.

## References

1. Ashat, A., Ardiansyah, F. (2012). Igniting the ring of fire: A Vision for Developing Indonesia's Geothermal Power. *WWF report*.
2. Bertani, R. (2012). Geothermal power generation in the world 2005–2010 update report. *Geothermics*, 41(3), 1–29. DOI 10.1016/j.geothermics.2011.10.001.
3. Babajide, O., Musyoka, N., Petrik, L., Ameer, P. (2012). Novel zeolite Na-X synthesized from fly ash as a heterogeneous catalyst in biodiesel production. *Catalysis Today*, 190(1), 54–60. DOI 10.1016/j.cattod.2012.04.044.
4. Cheung, O., Hedin, N. (2014). Zeolites and related sorbents with narrow pores for CO<sub>2</sub> separation from flue gas. *RSC Advances*, 4(28), 14480–14494. DOI 10.1039/C3RA48052F.
5. Fan, Y., Zhang, F. S., Zhu, J., Liu, Z. (2008). Effective utilization of waste ash from MSW and coal co-combustion power plant—zeolite synthesis. *Journal of Hazardous Materials*, 153(1–2), 382–388. DOI 10.1016/j.jhazmat.2007.08.061.
6. Kamali, M., Vaezifar, S., Kolahduzan, H., Malekpour, A., Abdi, M. R. (2009). Synthesis of nanozeolite A from natural clinoptilolite and aluminum sulfate: Optimization of the method. *Powder Technology*, 189(1), 52–56. DOI 10.1016/j.powtec.2008.05.015.
7. Machado, N. R. C. F., Miotto, D. M. M. (2005). Synthesis of Na-A and -X zeolites from oil shale ash. *Fuel*, 84(18), 2289–2294. DOI 10.1016/j.fuel.2005.05.003.
8. Deng, L. L., Xu, Q. Y., Wua, H. N. (2016). Synthesis of zeolite-like material by hydrothermal and fusion methods using municipal solid waste fly ash. *Procedia Environmental Sciences*, 31(1), 662–667. DOI 10.1016/j.proenv.2016.02.122.
9. Fukasawa, T., Karisma, A. D., Shibata, D., Huang, A. N., Fukui, K. (2017). Synthesis of zeolite from coal fly ash by microwave hydrothermal treatment with pulverization process. *Advanced Powder Technology*, 28(3), 798–804. DOI 10.1016/j.appt.2016.12.006.
10. Santasnachoka, C., Kurniawana, W., Hinodea, H. (2015). The use of synthesized zeolites from power plant rice husk ash obtained from Thailand as adsorbent for cadmium contamination removal from zinc mining. *Journal of Environmental Chemical Engineering*, 3(3), 2115–2126. DOI 10.1016/j.jece.2015.07.016.
11. Eng-Poh, N., Awala, H., Kok-Hou, T., Adama, F., Retoux, R. et al. (2015). EMT-type zeolite nanocrystals synthesized from rice husk. *Microporous and Mesoporous Materials*, 204, 204–209. DOI 10.1016/j.micromeso.2014.11.017.
12. Sulardjaka, Nugroho, S., Fitriyana, D. F. (2014). Synthesis of zeolite from geothermal waste. *Applied Mechanics and Materials*, 660, 157–161. DOI 10.4028/www.scientific.net/AMM.660.157.
13. Aidan, M. D., Roxana, P., David, S., Roger, R., Lubomira, T. (2019). Methane oxidation over zeolite catalysts prepared from geothermal fluids. *Microporous and Mesoporous Materials*, 2851, 56–60.
14. Widayat, Hadiyanto, Satriadi, H., Cahyono, B., Astuti, W. I. S. T. et al. (2019). Synthesis of zeolite x molecular sieve from geothermal solid waste—sciencedirect. *Materials Today: Proceedings*, 13(1), 137–142. DOI 10.1016/j.matpr.2019.03.203.
15. Munfarida, S., Widayat, Satriadi, H., Cahyono, B., Prameswari, J. (2020). Geothermal industry waste-derived catalyst for enhanced biohydrogen production. *Chemosphere*, 258, 127274. DOI 10.1016/j.chemosphere.2020.127274.
16. Silvia, S., Roxana, P. F., Javier, G., Benigno, S., Roger, R. et al. (2020). Silicalite-1 synthesized with geothermal and Ludox colloidal silica and corresponding TiO<sub>2</sub>/silicalite-1 hybrid photocatalysts for VOC oxidation. *Microporous and Mesoporous Materials*, 302(1), 1–8.

17. Liu, Z., Wang, Y., Dong, H. (2001). Synthesis of detergent-used zeolite 4A from montmorillonite. *Journal of Nanjing University (Natural Science)*, 1, 97–103.
18. Motuzas, J., Julbe, A., Noble, R. D., Guizard, C., Beresnevicius, Z. J. et al. (2005). Rapid synthesis of silicalite-1 seeds by microwave assisted hydrothermal treatment. *Journal of Microporous and Mesoporous Material*, 80(1–3), 73–83. DOI 10.1016/j.micromeso.2004.12.002.
19. Wang, J., Li, D., Ju, F., Han, L., Bao, W. (2015). Supercritical hydrothermal synthesis of zeolites from coal fly ash for mercury removal from coal derived gas. *Fuel Processing Technology*, 136, 96–105. DOI 10.1016/j.fuproc.2014.10.020.
20. Shen, S. H., Zhang, S. G., Wang, D. W. (2001). Synthesis of zeolite A in hydrothermal system of acid-treated stellerite-NaOH-NaAlO<sub>2</sub>-H<sub>2</sub>O. *Journal of the Chinese Ceramic Society*, 5, 451–454.
21. Cundy, C., Forrest, J. O., Plaisted, R. J. (2003). Some observations on the preparation and properties of colloidal silicalites. Part I: Synthesis of colloidal silicalite-1 and titanosilicalite-1 (TS-1). *Microporous and Mesoporous Materials*, 66(2–3), 143–156. DOI 10.1016/j.micromeso.2003.08.021.
22. Katsuki, H., Furuta, S., Komarneni, S. (2001). Microwave versus conventional-hydrothermal synthesis of nay zeolite. *Journals of Porous Materials*, 8(1), 5–12. DOI 10.1023/A:1026583832734.
23. Chu, P., Dwyer, F. G., Vartuli, J. C. (1998). Crystallization method employing microwave radiation and its application in zeolite synthesis. U.S. Patent 4,778,666.
24. Slangen, P. M., Jansen, J. C., Bekkum, H. V. (1997). The effect of ageing on the microwave synthesis of zeolite NaA. *Journal of Microporous Material*, 9(5–6), 259–265. DOI 10.1016/S0927-6513(96)00119-8.
25. Bonaccorsi, L., Proverbio, E. (2008). Influence of process parameters in microwave continuous synthesis of zeolite LTA. *Journal of Microporous and Mesoporous Material*, 112(1–3), 481–493. DOI 10.1016/j.micromeso.2007.10.028.
26. Munfarida, S., Widayat, Satriadi, H., Cahyono, B. Hadiyanto et al. (2020). Geothermal industry waste-derived catalyst for enhanced biohydrogen production. *Chemosphere*, 258, 127274. DOI 10.1016/j.chemosphere.2020.127274.
27. Kazemia, A., Faghihi-Sani, M. A., Alizadeh, H. R. (2013). Investigation on cristobalite crystallization in silica-based ceramic cores for investment casting. *Journal of the European Ceramic Society*, 33(15–16), 3397–3402. DOI 10.1016/j.jeurceramsoc.2013.06.025.
28. Sulardjaka, Fitriana, D. F. (2017). The effect of concentration of NaOH and holding time on characteristic of zeolite synthesized from geothermal waste. *Reaktor*, 17(1), 17–24. DOI 10.14710/reaktor.17.1.17-24.
29. Ding, L., Yang, H., Rahimi, P., Omotoso, O., Friesen, W. et al. (2010). Solid transformation of zeolite NaA to sodalite. *Microporous and Mesoporous Materials*, 130(1–3), 303–308. DOI 10.1016/j.micromeso.2009.11.025.
30. Wakihara, T., Sugiyama, A., Okubo, T. (2004). Crystal growth of faujasite observed by atomic force microscopy. *Microporous and Mesoporous Material*, 70(1–3), 7–13. DOI 10.1016/j.micromeso.2004.02.016.
31. Smilgies, D. M. (2009). Scherrer grain-size analysis adapted to grazing-incidence scattering with area detectors. *Journal of Applied Crystallography*, 42(6), 1030–1034. DOI 10.1107/S0021889809040126.
32. Parmar, R., Mangrola, M. H., Parmar, B. H., Joshi, V. G. (2012). A software to calculate crystalline size by Debye-Scherrer Formula using VB.NET. *Multi Disciplinary Edu Global Quest*, 1(1), 33–39.
33. Alfaro, S., Rodríguez, C., Valenzuela, M. A., Bosch, P. (2007). Aging time effect on the synthesis of small crystal LTA zeolites in the absence of organic template. *Materials Letters*, 61(23–24), 4655–4658. DOI 10.1016/j.matlet.2007.03.009.
34. Girnus, I., Jancke, K., Vetter, R., Richter-Mendau, J., Caro, J. (1995). Large AIPO<sub>4</sub>-5 crystals by microwave heating. *Zeolites*, 15(1), 33–39. DOI 10.1016/0144-2449(94)00004-C.
35. Ansari, M., Aroujalian, A., Raisi, A., Dabir, B., Fathizadeh, M. (2014). Preparation and characterization of nano-NaX zeolite by microwave assisted hydrothermal method. *Advanced Powder Technology*, 25(2), 722–727. DOI 10.1016/j.appt.2013.10.021.